Monte Carlo Calculation of Absorbed Dose Under MeV Proton Irradiation

Hiwa Mohammad Qadr*, Dyari Mustafa Mamand

University of Raparin, College of Science, Department of Physics, Sulaymaniyah, Iraq
e-mail: corresponding author hiwa.physics@uor.edu.krd

ABSTRACT

The primary aim of this evaluation is to define the radiation level on performing the measurement quantitatively. Three different methods were applied during this process, including simulating by FORTRAN code, measuring by Geiger Muller Counter and calculating with the activity data we had obtained. The simulation provided us an initial value range the radiation would lie in prior to our real operation. It acted as a guide. Measuring the dose rate by handheld Geiger Muller Counter provided the real radiation level during the experiment and can be used to reconfirm the safety condition of the experiment attendant. However, due to the fact that only a copper sample from 9 MeV was detected by the Geiger Muller Counter, the situation for other energy levels would be predicted by the calculation attempt. We also tried to build a calculation method that could be used more widely.

1- Introduction

Although neutron irradiation will always be necessary to test materials for reactor applications, ion beams can provide a lower cost and rapid mechanism for various purposes. Ion irradiation can be any charged particle beam, including electrons, protons or heavier nuclei [1-11]. One of the great advantages of ion irradiation is that it can be conducted for specific energy, dose rate and temperature, leading to a well-controlled experiment. Furthermore, ion irradiation allows easy variation of these parameters over a wide range of values. Whereas, neutron experiments, conducted in test reactors, can be very unspecific due to the variety of neutron kinetic energies inside the reactor [12-21]. Additionally, the damage accumulation reached in ion irradiation is much higher than neutron ones. For instance, during a typical neutron irradiation experiment in a thermal test reactor, the end-of-life damage is 3-5dpa/year, likewise a fast reactor gives 20dpa/year. The average of end-of-life damage for components of a BWR core is 10 dpa, for PWR it is 80 dpa and for Advanced Fast Reactor it is 200 dpa [22-25]

The computational simulation used was made with the FORTRAN programming language in which is only compatible with a Linux operating system. The simulation takes into account target material properties and several incident beam parameters. The formulas used within the code that use these parameters could be used manually to calculate the activity. However, as the interaction probability cross sections are a function of incident beam energy this leads to a demanding computation. This is because the cross-section values would change as the proton through the specimen losing energy. This is the advantage of a computer simulation as now the heavy computations can be easily processed [26-32].

In this work, simulation was carried out to predict radioactivity. FORTRAN code was used for this simulation. The former one provided us with EXYZ file which representing how the protons would be distributed after interacting with the matter. Then after the EXYZ file was input into the FORTRAN code, which contains other database such as cross sections. The output of this code contains various files consisting of activity and dose etc. Activity was modelled using a code in the FORTRAN language. This was used to predict dose rate at a distance and activity at depth and isotopes that were produced.

2- Monte Carlo Simulation

One interesting feature of the FORTRAN code was that it would give an output of the predicted dose for an 80 Kg human standing 1m from the activated sample for one hour assuming there was 100% absorption of all incident radiation

across $1m^2$ of skin. This seemed quite relevant to the experiment and hence we could not only model the activity, but the dose the team might receive from the activation for the sample whilst performing the experiment. Dose was modelled across a range of times after irradiation: 1, 3, 24 and 48 hours for 1 and 2 weeks. This was then repeated for each of the three highest beam energies, 9, 20 and 30 MeV

that were used in this work, and the results are shown in figure 1. Unfortunately, this could not be done for the lower energies due to the lack of complete cross-section data. However, the dose from the higher beam energies is far more substantial than the lower ones. Therefore, this was not too concerning because compared to the high energy samples the low ones were negligible.
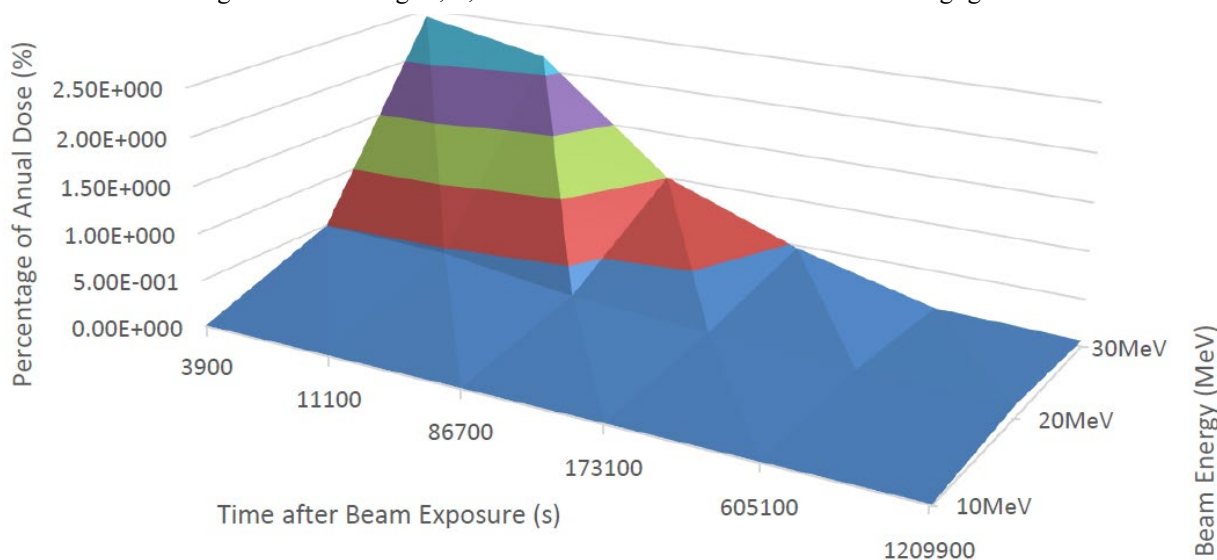

Figure 1. Modelled dose from FORTRAN

Figure 1 can be used to determine when various energy levels should be safe to measure. As one can see that the Dose is given as a percentage of the annual dose rate for a member of the public. If one took 1 hour as a percentage of a year, it equates to 0.0114 %, so logically the samples would be safe to handle when the percentage reaches this level. However, whilst this level would be safe, it would prevent meaningful measurements from being taken because so many of the isotopes would have decayed in this time due to many of them having short half-lives. Hence, if this limit was extended to 24 hours for example the safe percentage would be 0.274%. This would be an acceptable time as a compromise between safety and science because valid results could be taken and although the dose rate would not be safe for constant exposure it could be managed. This management would involve team members limiting their

time in the laboratory such that they are not exposed to this high dose rate too frequently and the dose would be averaged by the background radiation outside the laboratory which would be much lower than the accepted safe limit.

3. Measurement

The measurement was completed by handheld Geiger Muller Counter during the work process for the sample irradiated by 9 MeV protons. The result has clearly shown two types of decay in terms of time and distance, respectively. The significant reduction caused by increasing distance is proof that our practice including keeping distance from the source, using tweezers on moving sources, etc. was reliable. Figure 2 shows measured dose rate for 9 MeV irradiated sample.
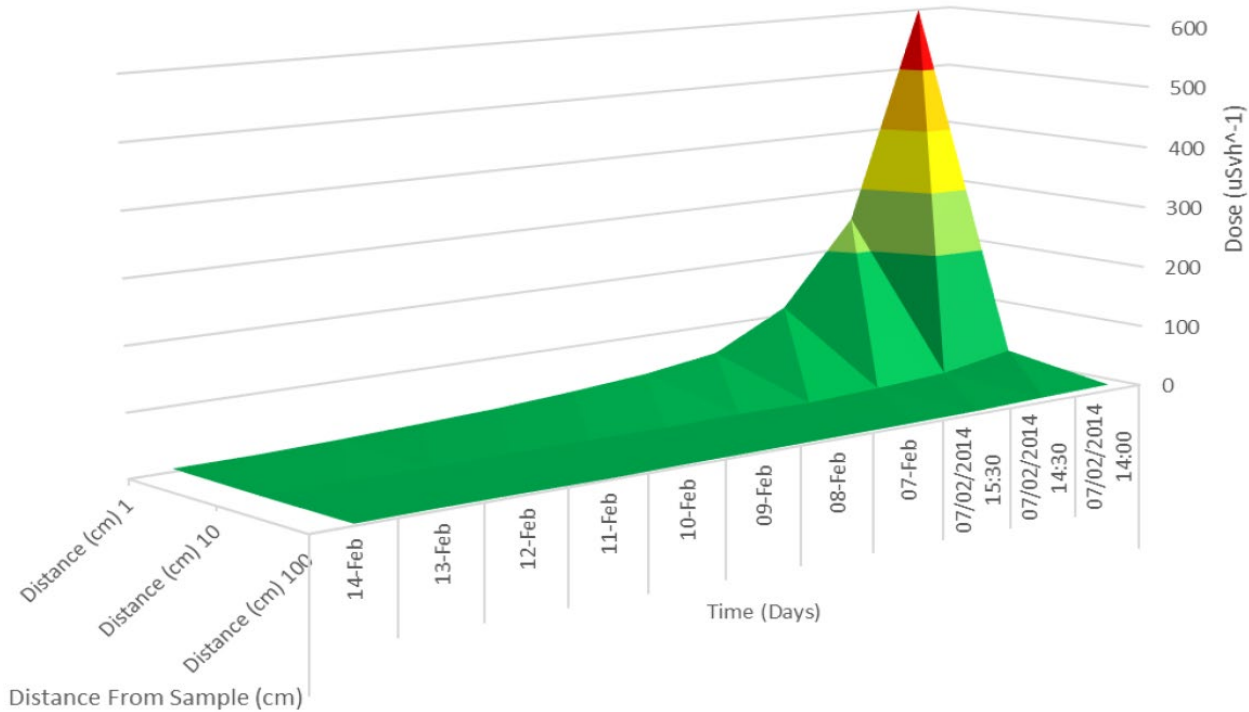
Figure 2. Measured dose rate for 9 MeV irradiated sample

4. Calculation

The method was developed based on the idea of converting the activity decay to dose decay. An equivalent dose was investigated and this value can be deduced from the absorbed dose as follows [33]:

$$H_T = \sum W_T \, D_{T,R} v \qquad (1)$$

Where W_T is the radiation weighting factor. For our situation that all the radiation considered was gamma rays, W_T has the value of 1. $D_{T,R}$ is the absorbed dose and can be calculated in the following equation [33]:

$$D = \frac{d\bar{\varepsilon}}{dm} \qquad (2)$$

Where $d\bar{\varepsilon}$ is the mean energy imparted into the matter of mass dm. In our work, equation (2) could be written as:

$$D = \Psi \frac{\mu_{en}}{\rho} \qquad (3)$$

Where Ψ is the energy fluence and $\frac{\mu_{en}}{\rho}$ is the mass attenuation coefficient, the equation could be further derived to be:

$$\Psi = E.A \frac{\Omega}{4\pi} \qquad (4)$$

Where E is the energy of radiation, A is the activity and Ω is the solid angle from the human body to the source. The expression for different energy gamma rays can be obtained as [34]:

$$H = \sum E_i . A \frac{\Omega}{4\pi} . \frac{\mu_{en}}{\rho} \qquad (5)$$

Therefore, we can use the data obtained from the detector and make an evaluation of the dose rate.

In practice, the spectrum is continuous and calculation demand appeared too much to be possible. Life was made easier by selecting significant peaks from the spectrum and applying them in the calculating process. This approximation leads to the fact that the result of this calculation is a (net) value that only comes from the radiation of the sample. Background radiation was not taken into the final result. Figure 3 shows dose ray decay for a high copper sample at 9 MeV
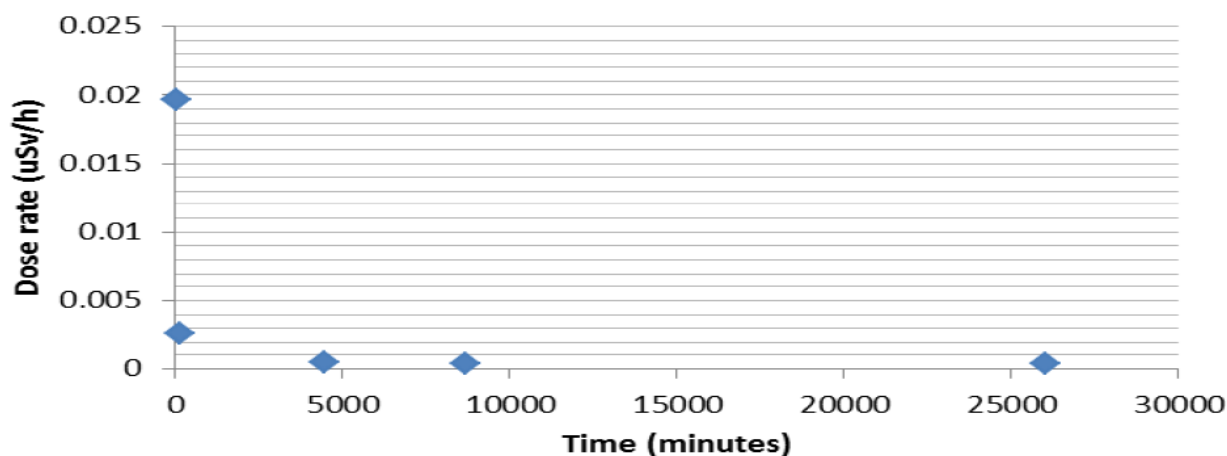
Figure 3. Dose ray decay for a high copper sample at 9 MeV

5. Comparison and conclusion

Now consider the match level of the result from this method to the measuring result. The main difference comes from the background radiation. When the sample was newly irradiated and had relatively strong radiation, the background term was not the main attribution to the total result. However, when the radiation from the sample decayed, the background radiation became the main attribution to the final result gradually. For the fact that most of our produced isotopes had a fairly short half-life, background radiation was the main attribution to the final result most time. This is confirmed by the above figure, in which the radiation dose from the sample was much lower than the general value.

This conclusion indicates that most time in our work, the real concerning point should be the background radiation. Our counterplan is staying in the detecting room as little as possible, for instance waiting in the general stuff room or corridor during the detecting process. Radiation in these places was much lower than that in the detecting room according to the Geiger Muller Counter.

References

[1] M.Q. Hiwa, *The use of the MCNP Code for Radiation Damage Calculations*, Mathematical Physics and Computer Modeling 24(1) (**2021**). https://doi.org/10.15688/mpcm.jvolsu.2021.1.5

[2] T. Muroga, M. Gasparotto, S.J. Zinkle, *Overview of materials research for fusion reactors*, Fusion engineering and design 61 (**2002**) 13-25.

[3] H.M. Qadr, *Radiation damage and dpa in iron using mcnp5*, European Journal of Materials Science and Engineering 5(3) (**2020**) 109-114.

[4] S.H. Park, J.O. Kang, *Basics of particle therapy I: physics*, Radiation oncology journal 29(3) (**2011**) 135.

[5] D.M. Mamand, A.H. Awla, T.M.K. Anwer, H.M. Qadr, *Quantum chemical study of heterocyclic organic compounds on the corrosion inhibition*, Chimica Techno Acta 9(2) (**2022**) 20229203. https://doi.org/10.15826/chimtech.2022.9.2.03

[6] D.M. Mamand, H.H. Rasul, P.K. Omer, H.M. Qadr, *Theoretical and experimental investigation on ADT organic semiconductor in different solvents*, Kondensirovannye sredy i mezhfaznye granitsy= Condensed Matter and Interphases 24(2) (**2022**) 227-242. https://doi.org/10.17308/kcmf.2022.24/9263

[7] H.M. Qadr, *Calculation for gamma ray buildup factor for aluminium, graphite and lead*, International Journal of Nuclear Energy Science and Technology 13(1) (**2019**) 61-69.

[8] H.M. Qadr, *Proportional Counter in X-Ray Fluorescence*, Aksaray University Journal of Science and Engineering 5(1) (**2021**) 1-7.

[9] H.M. Qadr, A.M. Hamad, *MECHANICAL PROPERTIES OF FERRITIC MARTENSTIC STEELS: A REVIEW*, Scientific Bulletin of'Valahia'University. Materials & Mechanics 17(16) (**2019**).

[10] H.M. Qadr, *Experimental Study of the Pressure Effects on Stopping Power for Alpha Particles in Air*, Gazi University Journal of Science (**2022**) 272-279.

[11] I.N. Qader, H.M. Qadr, P.H. Ali, *Calculation of Lattice Thermal Conductivity for Si Fishbone Nanowire Using Modified Callaway Model*, Semiconductors 55(12) (**2021**) 960-967. 10.1134/S1063782621070137

[12] H.M. Qadr, *Effect of ion irradiation on the mechanical properties of high and low copper*, Atom Indonesia 46(1) (**2020**) 47-51. https://doi.org/10.17146/aij.2020.923

[13] H.M. Qadr, *A molecular dynamics calculation to cascade damage processes*, The Annals of "Dunarea de Jos" University of Galati. Fascicle IX, Metallurgy and Materials Science 43(4) (**2020**) 13-16. https://doi.org/10.35219/mms.2020.4.02

[14] H.M. Qadr, *A Molecular Dynamics Study of Temperature Dependence of the Primary State of Cascade Damage Processes*, Russian Journal of Non-Ferrous Metals 62(5) (**2021**) 561-567. https://doi.org/10.3103/S1067821221050096

[15] H.M. Qadr, *Pressure Effects on Stopping Power of Alpha Particles in Argon Gas*, Physics of Particles and Nuclei Letters 18(2) (**2021**) 185-189. https://doi.org/10.1134/S1547477121020151

[16] H.M. Qadr, D.M. Mamand, *Molecular Structure and Density Functional Theory Investigation Corrosion Inhibitors of Some Oxadiazoles*, Journal of Bio- and Tribo-Corrosion 7(4) (**2021**) 140. https://doi.org/10.1007/s40735-021-00566-9

[17] H.M. Qadr, *Comparison of energy resolution and efficiency of NaI (TI) and HPGe detector using gamma-ray spectroscopy*, Journal of Physical Chemistry and Functional Materials 3(1) (**2020**) 24-27.

[18] M.C. Almeida, A.A. Steiner, L.G.S. Branco, A.A. Romanovsky, *Cold-seeking behavior as a thermoregulatory strategy in systemic inflammation*, European Journal of Neuroscience 23(12) (**2006**) 3359-3367.

[19] M. Dyari Mustafa, Q. Hiwa Mohammad, *Comprehensive Spectroscopic and Optoelectronic Properties of BBL Organic Semiconductor*, Protection of Metals and Physical Chemistry of Surfaces 57(5) (**2021**) 943-953. https://doi.org/10.1134/S207020512105018X

[20] A.M. Hamad, H.M. Qadr, *Gamma-rays spectroscopy by using a thallium activated sodium iodide NaI (Ti)*, Eurasian Journal of Science and Engineering 4(1) (**2019**) 99-111.

[21] M.Q. Hiwa, *Stopping power of alpha particles in helium gas*, Bulletin of the Moscow State Technical University NE Bauman Series "Natural Sciences" https://doi.org/10.18698/1812-3368-2020-2-117-125(2 (89)) (**2020**) 117-125.

[22] G.S. Was, R.S. Averback, Radiation damage using ion beams, Comprehensive Nuclear Materials, Elsevier Ltd2012, pp. 195-221.

[23] J.M. Perlado, J. Sanz, Irradiation Effects and Activation in Structural Materials, Nuclear Fusion by Inertial Confinement, CRC Press2020, pp. 615-671.

[24] A. Bhattacharya, S. Zinkle, J. Henry, S.M. Levine, P.D. Edmondson, M.R. Gilbert, H. Tanigawa, C.E. Kessel, *Irradiation damage concurrent challenges with RAFM and ODS steels for fusion reactor first-wall/blanket: A review*, Journal of Physics: Energy (**2022**).

[25] H.M. Qadr, *An exploration into wind turbines, their impacts and potential solutions*, Journal of Environmental Science and Public Health 2(1) (**2018**) 64-69.

[26] D.H. Bailey, *A Fortran 90-based multiprecision system*, ACM Transactions on Mathematical Software (TOMS) 21(4) (**1995**) 379-387.

[27] H.M. Qadr, *Effect of ion irradiation on the hardness properties of Zirconium alloy*, Annals of the University of Craiova, Physics 29 (**2019**) 68-76.

[28] Q.H. Mohammad, H.A. Maghdid, *Using of stopping and range of ions in Matter code to study of radiation damage in materials*, Rensit 12(4) (**2020**) 451-456. https://doi.org/10.21517/0202-3822-2020-43-2-25-30

[29] H.M. Qadr, D. Mamand, *A Review on DPA for computing radiation damage simulation*, Journal of Physical Chemistry and Functional Materials 5(1) (**2022**) 30-36.

[30] M.Q. Hiwa, M.H. Ari, *Investigation of long and short term irradiation hardening of P91 and P92 ferritic/martensitic steels*, Problems of Atomic Science and Technology. Series:Thermonuclear Fusion 42(2) (**2019**) 81-88.

[31] H.M. Qadr, *Calculation of gamma-ray attenuation parameters for aluminium, iron, zirconium and tungsten*, Problems of Atomic Science and Technology. Series:Thermonuclear Fusion 43(2) (**2020**) 25-30.

[32] Q. Mohammad, H. Maghdid, *Alpha- particle stopping powers in air and argon*, Journal of pure and applied physics 5 (**2017**) 22-28.

[33] R. Protection, *ICRP publication 103*, Ann ICRP 37(2.4) (**2007**) 2.

[34] E. Cléro, L. Vaillant, N. Hamada, W. Zhang, D. Preston, D. Laurier, N. Ban, *History of radiation detriment and its calculation methodology used in ICRP Publication 103*, Journal of Radiological Protection 39(3) (**2019**) R19.